THE JOURNAL OF BIOLOGICAL CHEMISTRY
Vol. 274, No. 15, Issue of April 9, pp. 10324–10330, 1999

Printed in U.S.A.

Description of a Versatile Peroxidase Involved in the Natural Degradation of Lignin That Has Both Manganese Peroxidase and Lignin Peroxidase Substrate Interaction Sites*

(Received for publication, September 15, 1998, and in revised form, December 21, 1998)

Susana Camarero, Sovan Sarkar‡, Francisco Javier Ruiz-Dueñas, María Jesús Martínez, and Ángel T. Martínez§

From the Centro de Investigaciones Biológicas, Consejo Superior de Investigaciones Científicas, Velázquez 144, E-28006 Madrid, Spain

Two major peroxidases are secreted by the fungus *Pleurotus eryngii* in lignocellulose cultures. One is similar to *Phanerochaete chrysosporium* manganese-dependent peroxidase. The second protein (PS1), although catalyzing the oxidation of Mn^{2+} to Mn^{3+} by H_2O_2, differs from the above enzymes by its manganese-independent activity enabling it to oxidize substituted phenols and synthetic dyes, as well as the lignin peroxidase (LiP) substrate veratryl alcohol. This is by a mechanism similar to that reported for LiP, as evidenced by *p*-dimethoxybenzene oxidation yielding benzoquinone. The apparent kinetic constants showed high activity on Mn^{2+}, but methoxyhydroquinone was the natural substrate with the highest enzyme affinity (this and other phenolic substrates are not efficiently oxidized by the *P. chrysosporium* peroxidases). A three-dimensional model was built using crystal models from four fungal peroxidase as templates. The model suggests high structural affinity of this versatile peroxidase with LiP but shows a putative Mn^{2+} binding site near the internal heme propionate, involving Glu^{36}, Glu^{40}, and Asp^{181}. A specific substrate interaction site for Mn^{2+} is supported by kinetic data showing noncompetitive inhibition with other peroxidase substrates. Moreover, residues reported as involved in LiP interaction with veratryl alcohol and other aromatic substrates are present in peroxidase PS1 such as His^{82} at the heme-channel opening, which is remarkably similar to that of *P. chrysosporium* LiP, and Trp^{170} at the protein surface. These residues could be involved in two different hypothetical long range electron transfer pathways from substrate (His^{82}-Ala^{83}-Asn^{84}-His^{47}-heme and Trp^{170}-Leu^{171}-heme) similar to those postulated for LiP.

The biodegradation of lignin represents a key step for carbon recycling on earth because forest ecosystems contain about 150,000 million tons of wood (1). Although the main wood constituent, cellulose, can be utilized by a variety of organisms, its hydrolysis *in situ* by most of them is hampered by the recalcitrant lignin polymer, which is formed by polymerization of plant *p*-hydroxycinnamyl alcohols (2). However, the so-called white rot fungi, a group of species from class Basidiomycetes, have developed a remarkable capability for oxidative depolymerization and subsequent mineralization of lignin (3) enabling cellulose utilization by other organisms.

During recent years many studies on lignin biodegradation have been carried out in the fungus *Phanerochaete chrysosporium* (order Stereales). The first evidence of peroxidase involvement came from inhibition of lignin degradation by catalase (4). Then two peroxidases involved in lignin degradation, the so-called lignin peroxidase (LiP)[1] and manganese peroxidase or manganese-dependent peroxidase (MnP), were described (5–7). LiP is characterized by high redox potential enabling oxidation of hardly biodegradable nonphenolic aromatic compounds, such as veratryl alcohol and methoxylated benzenes. *P. chrysosporium* MnP strictly requires Mn^{2+} to complete the catalytic cycle, and the chelates of Mn^{3+} formed can act as efficient oxidizers of phenols and other compounds. Because most units in lignin are nonphenolic (2), LiP was considered as the main enzyme responsible for lignin depolymerization (3). This is still generally accepted, although some evidence suggests that lignin biodegradation could proceed by endwise attack at the phenolic units (8) and that, in addition to Mn^{3+} chelates, strong chemical oxidants can be generated by MnP (9).

Since 1983–1984 a large amount of information on peroxidases from *P. chrysosporium* has been accumulated (10–13), and crystal models have been described (14–16). At the time of the LiP model, only the cytochrome *c* peroxidase crystal structure was available. The information on their molecular structure not only clarified some peculiarities of these enzymes but also contributed to better understanding of some aspects of peroxidase structure and function (17). Despite the above progresses, the mechanism by which lignin is biodegraded is still to be fully understood, and only a limited number of biotechnological applications have been developed. This is related to the fact that the above studies have been focused on a single organism and that little is known about lignin degradation by fungi in their natural environment. Studies on lignocellulose degradation under solid state fermentation (SSF) conditions, which are close to those of natural habitat of white rot fungi, should provide information to contrast that obtained using liquid media (18–20).

* This work was supported by European Contract AIR2-CT93-1219 and Project BIO96-393 of the Spanish Biotechnology Programme. The costs of publication of this article were defrayed in part by the payment of page charges. This article must therefore be hereby marked "*advertisement*" in accordance with 18 U.S.C. Section 1734 solely to indicate this fact.

The atomic coordinates and structure factors (code 1BQW) have been deposited in the Protein Data Bank, Brookhaven National Laboratory, Upton, NY.

‡ Present address: University of Westminster, Div. of Biotechnology, 115 New Cavendish St., W1M 8JS London, UK.

§ To whom correspondence should be addressed. Tel.: 34915611800; Fax: 34915627518; E-mail: cibm149@fresno.csic.es; URL address: http://www.cib.csic.es/~lignina/lignina_en.html.

[1] The abbreviations used are: LiP, lignin peroxidase; AAO, aryl-alcohol oxidase; ABTS, 2,2′-azinobis(3-ethylbenzothiazoline-6-sulfonate); ARP, *Arthromyces ramosus* peroxidase; CIP, *Coprinus cinereus* peroxidase; LRET, long range electron transfer; MnP, manganese peroxidase; SSF, solid state fermentation; HPLC, high pressure liquid chromatography.

The fungus *Pleurotus eryngii* (order Poriales) has been reported as having the capability to remove lignin selectively when growing on natural substrates and is therefore considered a model organism for studies on biodegradation of lignin in annual plants and related biotechnological applications (21, 22). Peroxidases oxidizing Mn^{2+} have been reported in liquid cultures of *P. eryngii* (23), together with the AAO responsible for H_2O_2 generation in *Pleurotus* species and laccases (21, 24). However, no typical LiP has been described in this or other *Pleurotus* species. The aim of the present study was to identify and characterize the peroxidases involved in natural degradation of lignin by this fungus and to investigate the eventual production of LiP. *P. eryngii* was therefore grown on a lignocellulosic substrate under SSF conditions, and several peroxidases were isolated. Their catalytic properties were investigated using different substrates, and a three-dimensional model for a *P. eryngii* peroxidase was built using existing crystal models from other fungal peroxidases as templates.

EXPERIMENTAL PROCEDURES

Organisms and Culture Conditions—*P. eryngii* ATCC 90787 (IJFM A169), *Trametes versicolor* IJFM A136, and *P. chrysosporium* ATCC 24725 (VKM F-1767) were grown on sterile wheat straw under SSF conditions. These are characterized by the presence of enough liquid phase to saturate the solid lignocellulosic substrate, maintaining an air phase between particles. The fungi were grown in an horizontal rotary fermentor, which included six 2-liter bottles containing 125 g of straw (length, 1–2 cm) and 375 ml of water (including inoculum). The inoculation and growth conditions were already described (22). Samples were taken during 2 months to analyze enzymatic activities and substrate degradation. Lignin content was estimated by the Klason method after Saeman's acid hydrolysis and polysaccharide composition by gas chromatography of the acid hydrolyzate, following T-222 and T249 rules (25).

Chemicals—Reactive Black 5 ($C_{26}H_{21}N_5O_{19}S_6Na_4$) was obtained from DyStar (Frankfurt, Germany), 2,2′-azinobis(3-ethylbenzothiazoline-6-sulfonate) (ABTS) was from Boehringer, and other chemicals were from Sigma-Aldrich.

Enzymatic Activities—LiP activity was assayed by oxidation of 2 mM veratryl alcohol to veratraldehyde (ϵ_{310} 9.3 mM^{-1} cm^{-1}) in 0.1 M tartrate buffer, pH 3, with 0.4 mM H_2O_2 (controls without H_2O_2 were included). Mn^{2+}-oxidizing peroxidase was estimated by formation of Mn^{3+} tartrate (ϵ_{238} 6.5 mM^{-1} cm^{-1}) from 0.1 mM $MnSO_4$ in 0.1 M sodium tartrate, pH 5, with 0.1 mM H_2O_2. Peroxidase activity on phenols was quantified using 2.5 mM syringol (2,6-dimethoxyphenol) (ϵ_{469} 27.5 mM^{-1} cm^{-1} referred to substrate), in 0.1 M sodium tartrate, pH 3, with 0.1 mM H_2O_2 (23). AAO was determined as the veratraldehyde formed from 5 mM veratryl alcohol in 0.1 M phosphate buffer, pH 6. Laccase was measured with 10 mM syringol in 0.1 M sodium tartrate, pH 5. One activity unit was defined as the amount of enzyme transforming 1 μmol of substrate/min.

Enzyme Purification—Peroxidases were purified from 15-day-old SSF cultures. Water extracts from the straw treated with the fungus were obtained (by adding 3 liters/bottle and shaking for 1 h at 200 rpm), filtered (0.8 μm), concentrated by ultrafiltration (5-kDa cut-off), and dialyzed against 10 mM sodium tartrate, pH 4.5. The concentrate (approximately 140 ml) was loaded onto a Bio-Rad Q-cartridge (1 ml/min), and retained fractions were eluted with 1 M NaCl. Fractions with peroxidase activity were concentrated, and 1-ml samples applied onto a Sephacryl S-200 HR column (0.8 ml/min). The peroxidase fractions were pooled, concentrated, and dialyzed against 10 mM sodium tartrate, pH 5, and 1-ml samples were applied to a Mono-Q column. Proteins with peroxidases activity were separated using a 0–0.25 M NaCl gradient (30 min, 0.8 ml/min).

Enzyme Characterization—Protein concentration was determined with the Bradford reagent. Isoelectric focusing was performed in 5% polyacrylamide gels with a thickness of 1 mm and a pH range from 2.5 to 5.5. SDS-polyacrylamide gel electrophoresis was carried out in 12% polyacrylamide gels. Gels were stained with Coomassie Blue R-250. Proteins were deglycosylated using Endo-H from Boehringer. The N-terminal sequences were obtained by automated Edman degradation of 5 μg of protein in an Applied Biosystems 494 pulsed liquid protein sequencer. The steady state kinetic constants were obtained from Lineweaver-Burk plots, and the mean values are presented. The kinetic constants for Mn^{2+} peroxidase activity were calculated by the formation of Mn^{3+} tartrate at pH 5. Manganese-independent activities at pH 3 on ABTS (cation radical ϵ_{436} 29.3 mM^{-1} cm^{-1}), Reactive Black 5 (ϵ_{558} 50 mM^{-1} cm^{-1}), guaiacol (*o*-methoxyphenol) (oxidation product ϵ_{456} 12.1 mM^{-1} cm^{-1} referred to substrate concentration), syringol, methoxyhydroquinone (methoxybenzoquinone ϵ_{360} 1.25 mM^{-1} cm^{-1}), veratryl alcohol, and *p*-dimethoxybenzene (benzoquinone ϵ_{254} 21 mM^{-1} cm^{-1}) were estimated in the presence of EDTA, and kinetic constants were calculated. The K_m for the enzyme-oxidizing substrate H_2O_2 was also obtained at pH 5 (by measuring Mn^{2+} oxidation) and pH 3 (syringol oxidation). Reciprocal inhibition between Mn^{2+} and Reactive Black 5 was investigated by following spectrophotometrically the effect of different concentrations of both compounds as inhibitors on the decolorization by peroxidase PS1 of 0.8–25 μM Reactive Black 5 (high concentration caused substrate inhibition) in 0.1 M sodium tartrate, pH 4, and the oxidation of 10–400 μM Mn^{2+} in 0.1 M sodium tartrate, pH 5 (all reactions contained 0.1 mM H_2O_2).

TABLE I
Extracellular enzymatic activities and fungal modification of lignocellulose composition

No peroxidase activity on veratryl alcohol (LiP) was detected, and maximal laccase, AAO, and Mn^{2+}-oxidizing peroxidase (MnP) activities are shown as units/100 g initial straw.

	MnP	AAO	Laccase	Polysaccharide/lignin ratio[a]
P. eryngii	300	4	66	4.4
P. chrysosporium	70	0	0	2.2
T. versicolor	20	0	12	2.5
Control wheat straw	0	0	0	2.6

[a] At the end of incubation period.

HPLC Analysis of p-Dimethoxybenzene Oxidation—The oxidation of *p*-dimethoxybenzene (1 mM) was followed spectrophotometrically, using 0.1 M sodium tartrate, pH 3, and 0.2 mM H_2O_2. Samples (20 μl) from the reaction mixture were analyzed by HPLC using a C18 column (Spherisorb S5ODS2) at 30 °C. A methanol/phosphoric acid (10 mM) gradient (consisting of 10% methanol for 10 min, 10–100% methanol in 6 min, 100% methanol for 4 min, 100–10% methanol in 0.5 min, and 10% methanol for 6.5 min) was used (1 ml/min). Dual wavelength and diode array detectors were used. Standard calibration curves were used for quantitation.

Protein Modeling—The atomic coordinates of crystal models of LiP-H8 (PDB entries 1LGA and 1LLP), LiP-H2 (1QPA), and MnP1 (1MNP) from *P. chrysosporium* and ARP-CIP (1ARP) were obtained from the Brookhaven Protein Data Base. The latter peroxidase has been crystallized from both *Coprinus cinereus* (CIP) (26) and *Arthromyces ramosus* (ARP) (27). Because the latter is an invalid species (*nomen nudum*), which could correspond to a *Coprinus* conidial state, and both proteins share 99% identity, the name ARP-CIP is used here for both of them. The gene coding for protein PS1 of *P. eryngii* has been cloned, and a preliminary sequence has been obtained (28). From the predicted amino acid sequence a three-dimensional model for the mature protein without Mn^{2+} was obtained by sequence homology using the program ProMod and refined by CHARMm (the C-terminal region was not modeled) (29). It was based on alignment of sequence of peroxidase PS1 with the above four fungal peroxidases for which crystal models are available. Secondary structure was determined with the DSSP program (30). The above models for *P. chrysosporium* MnP and LiP were also used for comparison with *P. eryngii* peroxidase PS1 using programs Swiss-Pdb Viewer and RasMol. Multiple sequence alignment was prepared with PILEUP from GCG package using W2H interface.

RESULTS

P. eryngii degrades wheat lignin maintaining high cellulose content. This resulted in the increased polysaccharide/lignin ratio shown in Table I. Preferential degradation of lignin is a singular characteristic because most ligninolytic basidiomycetes (including the *P. chrysosporium* and *T. versicolor* strains shown in Table I) cause stronger degradation of cellulose than lignin. When the presence of ligninolytic enzymes was investigated in the partially degraded straw no LiP was detected in any case, but AAO, laccase, and Mn^{2+}-oxidizing peroxidase were all produced by *P. eryngii* and *T. versicolor*. The high Mn^{2+}-oxidizing activity produced by *P. eryngii* suggested that the enzyme responsible for this activity could be involved in lignin degradation.

The process of peroxidase purification included ultrafiltration of the extract from SSF culture of *P. eryngii*, followed by Q-cartridge (removing colored compounds from lignin degradation), molecular size exclusion, and ion exchange chromatogra-

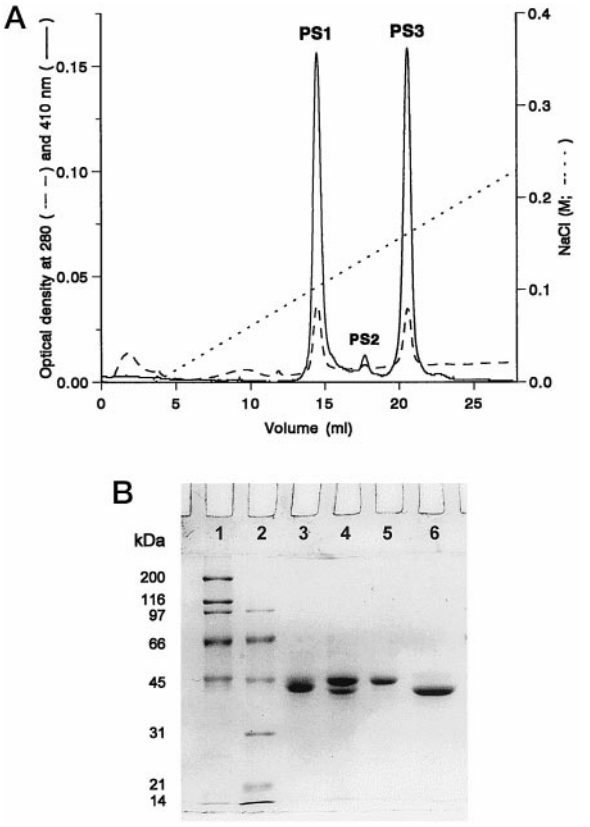

FIG. 1. **Purification of *P. eryngii* extracellular peroxidases from wheat-straw partially delignified by the fungus.** *A*, ion exchange chromatography. In the last purification step (Mono-Q chromatography at pH 5) two major and one minor proteins (PS1 to PS3) with high absorbance at 410 nm and peroxidase activity on different substrates were isolated from straw treated with the fungus under SSF conditions (410- and 280-nm profiles and NaCl gradient are shown). *B*, SDS-polyacrylamide gel electrophoresis. Peroxidases PS1 and PS3 are shown before (*lane 4*) and after Mono-Q separation (*lane 5*, PS1; *lane 6*, PS3) compared with peroxidase from liquid culture (*lane 3*) (23) (Coomassie Blue R-250 staining). *Lanes 1* and *2* correspond to high and low molecular mass standards.

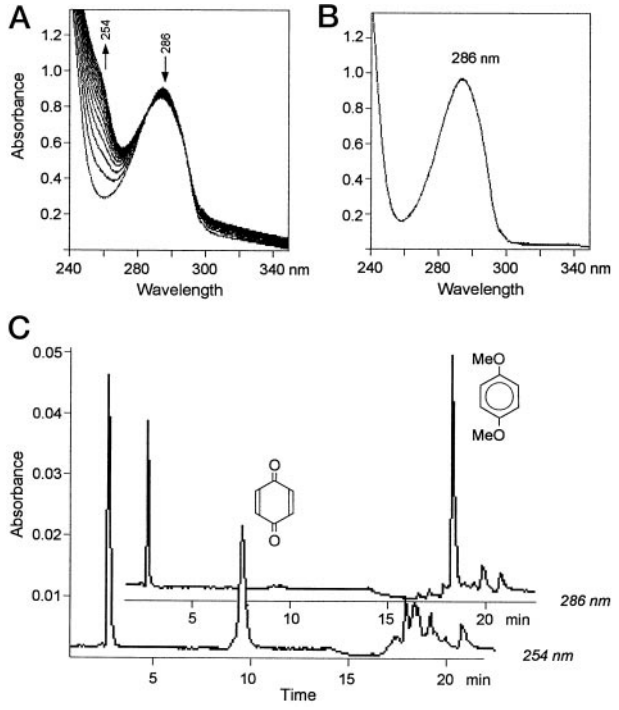

FIG. 2. **Assay of *p*-dimethoxybenzene oxidation by *P. eryngii* peroxidases PS1 and PS3.** *A*, peroxidase PS1. Substrate oxidation was evidenced by the increase in absorbance at 254 nm during incubation of 1 mM *p*-dimethoxybenzene with peroxidase PS1 (the reaction was in 0.1 M sodium tartrate, pH 3, using 0.2 mM H_2O_2; scans were recorded every 2 min; the molar absorbances of benzoquinone and *p*-dimethoxybenzene are ϵ_{254} 21 mM^{-1} cm^{-1}, and ϵ_{286} 0.98 mM^{-1} cm^{-1}, respectively). *B*, peroxidase PS3. The UV spectrum did not change under the same conditions described in *A* revealing that *p*-dimethoxybenzene is not oxidized by this enzyme. *C*, HPLC analysis (PS1). Benzoquinone formation after *p*-dimethoxybenzene incubation (20 min) with peroxidase PS1 was confirmed by HPLC using dual wavelength (254 and 286 nm) and diode array detectors, which enabled identification of the quinone formed (the benzoquinone UV spectrum is characterized by maximum at 254 nm) and quantitation of reaction substrate and product.

phy. As shown in Fig. 1*A*, the last purification step resulted in the isolation of two major protein peaks (labeled PS1 and PS3) and a minor one (protein PS2). Both major peaks were electrophoretically homogeneous (Fig. 1*B*) and were fully characterized. The three proteins exhibited high absorbance at 410 nm and were able to oxidize Mn^{2+} in the presence of H_2O_2. The optimum for this reaction was at pH 5. Proteins PS1, PS2, and PS3 differed in Mono-Q retention volume, A_{410}/A_{280} ratio (4.9, 4.9, and 5.5), isoelectric point (3.67, 3.65, and 3.80, respectively), molecular mass (45, 45, and 42 kDa, respectively), and N termini (VTCATGQTT for PS1 and PS2 and VTCADGNTV for PS3). In the case of protein PS1 a total of 25 amino acid residues were identified, and no double sequences were observed confirming protein purity. Proteins PS1 and PS3 also differed in the *N*-glycosylation degree (4 and 2%, respectively). A different Mn^{2+}-oxidizing peroxidase produced by *P. eryngii* when grown in liquid media (23) has a molecular mass intermediate between those of the two major peroxidases isolated here (Fig. 1*B*) and also differs in the N-terminal sequence.

In addition to their activity on Mn^{2+}, the peroxidases isolated from lignocellulose cultures were able to oxidize substituted phenols, such as guaiacol, syringol, and methoxyhydroquinone. The proteins PS1 and PS2 were able to also oxidize nonphenolic aromatic molecules such as the LiP substrate veratryl alcohol. The fact that peroxidase activity on veratryl alcohol (LiP-type activity) was not detected in the cultures (Table I) is probably due to its inhibition by phenols (or other aromatic compounds in extracts) as described for LiP (19;31). Because veratryl alcohol is a substrate of *Pleurotus* AAO (and can be oxidized by other fungal enzymes in the presence of mediators), *p*-dimethoxybenzene was assayed as a more specific LiP substrate. The results of incubation with peroxidases PS1 and PS3, only the first enzyme oxidizing the substrate, are shown in Fig. 2 (*A* and *B*). The HPLC analysis revealed benzoquinone as the reaction product by peroxidase PS1 (Fig. 2*C*). The higher redox potential of peroxidase PS1 was evidenced also by oxidation of some synthetic dyes. Whereas both enzymes oxidized ABTS (PS1 with 3-fold higher specific activity than PS3), only peroxidase PS1 was able to decolorize the Reactive Black 5, a high redox potential azo dye. The optimum for all the manganese-independent reactions was around pH 3.

The steady state kinetic constants of the two major peroxidases for oxidation of Mn^{2+} to Mn^{3+} and for manganese-independent oxidation of two phenolic and two nonphenolic aromatic substrates, and the dye Reactive Black 5 are shown in Table II. As already mentioned, the three latter substrates were oxidized only by peroxidase PS1, but both peroxidases also differed in the K_m values for the other substrates. These revealed higher affinities for Mn^{2+} and phenols of PS1 than PS3. Moreover, peroxidase PS1 could oxidize methoxyhydroquinone concentrations below 1 μM, whereas peroxidase PS3 did not exhibit activity below 100 μM substrate. The K_m obtained for peroxidase PS1 (17 μM) is lower than found for other enzyme-reducing aromatic substrates (with the only exception of synthetic dyes), revealing substituted

hydroquinones as the best natural substrates of *P. eryngii* peroxidase PS1 from the point of view of enzyme affinity. However, because of the higher turnover number for Mn^{2+} oxidation, both peroxidases showed the highest efficiency (t/K_m) for Mn^{2+} oxidation (even considering that oxidation of aromatic compounds should involve two one-electron oxidations). The apparent K_m values for H_2O_2, obtained during both Mn^{2+} oxidation at pH 5 and oxidation of aromatic substrates at pH 3, were low. This corresponds to high affinity of peroxidases for H_2O_2, but the value obtained at pH 3 could be considered as extremely low compared with other fungal peroxidases. Mutual inhibition between peroxidase PS1 oxidation of the substrates Reactive Black 5 (an azo dye that is not oxidized by Mn^{3+}) and Mn^{2+} was found. However, the azo dye appeared as a stronger inhibitor because the inhibitor/substrate molar ratio, to cause 40% inhibition, was 125 in the case of Mn^{2+} inhibition of dye oxidation, and only 0.13 in the case of Reactive Black 5 inhibition of Mn^{2+} oxidation. The type of inhibition caused by Reactive Black 5 was investigated using different dye concentrations, and although a decrease of the velocity of Mn^{2+} oxidation was found (the turnover number decreasing from 71 to 43 s^{-1} in the presence of 32 μM dye), the K_m value was maintained (around 50 μM). This suggests two different substrate interaction sites with different affinities that are not affected by the presence of the alternative substrate acting as inhibitor. The inhibitory effect would be caused by the reduction of the oxidized enzyme forms (compounds I and II) during oxidation of the substrate acting as inhibitor. Finally, it is possible to mention that the stronger inhibitory effect caused by Reactive Black 5 agrees with the higher peroxidase affinity for this substrate, compared with the affinity for Mn^{2+}.

TABLE II
Steady state kinetic constants of the two fungal peroxidases (PS1 and PS3) purified from straw partially delignified by P. eryngii (mean values)

	K_m		t	
	PS1	PS3	PS1	PS3
	μM		S^{-1}	
Mn^{2+} oxidation[a]				
Mn^{2+}	48	200	79	78
H_2O_2	9	10		
Manganese-independent reactions[b]				
Methoxyhydroquinone	17 (890)[c]	2530	4 (19)[c]	19
Syringol	200	1000	6	3
Veratryl alcohol	3500	0	4	0
p-Dimethoxybenzene	2400	0	4	0
Reactive Black 5	2	0	5	0
H_2O_2	2	3		

[a] pH 5.
[b] pH 3.
[c] A two-step activity curve was obtained when high substrate concentrations are used resulting in a second apparent K_m, the enzyme being more efficient at the lowest one.

Because the above results showed that peroxidase PS1 shared LiP and MnP-type catalytic properties, as well as some characteristics of other peroxidases oxidizing phenolic substrates, a three-dimensional model was built for the mature protein (this model includes the two helical domains characteristic of all peroxidases). The four fungal peroxidases for which crystal structures are available were used as templates for homology modeling, and a multiple alignment of their corresponding sequences together with the PS1 sequence that was modeled is shown in Fig. 3. These peroxidases are *P. chrysosporium* MnP1 (58% sequence identity with PS1) and isoenzymes H8 (60%) and H2 (62%) of LiP, and *Coprinus* ARP-CIP (52%). The model obtained showed good geometry with root mean square deviations in bond angles and distances of 2.31 ° and 0.013 Å, respectively. It includes 12 predominantly α helices, the position and size of which is indicated in Fig. 3. The helix B″corresponds to helix B′ of LiP (14), with both being longer than helix B′ of MnP1. A short helix at the position of helix B′ of *P. eryngii* peroxidase PS1 was described in ARP-CIP (27), and some helical conformation at this position can be observed also in LiP. Therefore, the three latter peroxidases could include 12 helices, compared with only 11 helices of *P. chrysosporium* MnP1. The peroxidase PS1 conserves some structurally important elements including disulphide bridges (the last one is not included in the model because it links the C-terminal region to helix I) and putative Ca^{2+} sites (distal Ca^{2+} linked by oxygens of Asp^{48}, Gly^{66}, Asp^{68}, and Ser^{70}; and proximal one by those of Thr^{176}, Asp^{193}, Thr^{195}, Thr^{198}, and Asp^{200}), characteristic of all peroxidases in classes II and III (17). The peroxidase PS1 model shows the highest coincidence in protein folding and helical topology and the lowest root mean

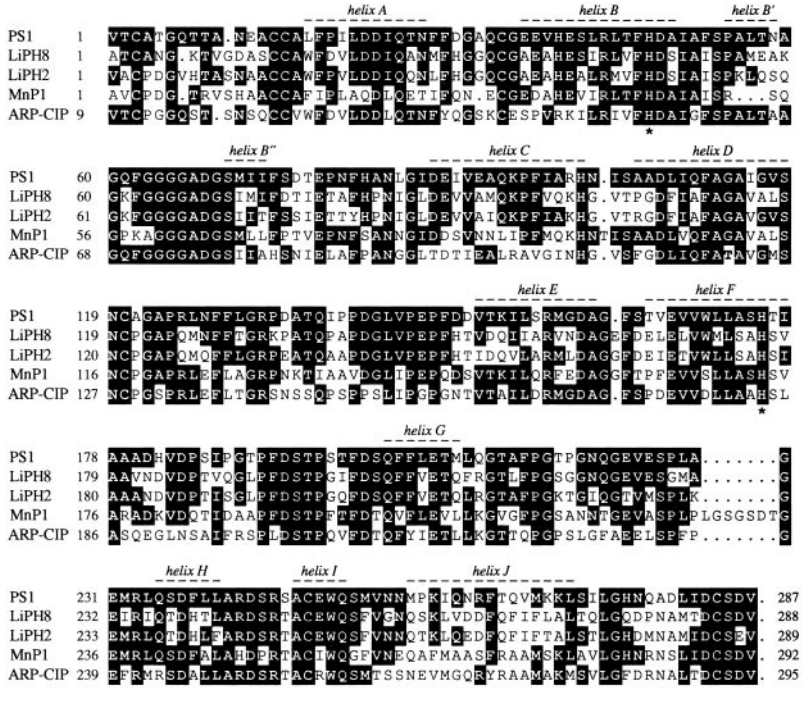

FIG. 3. **Multiple alignment of the amino acid sequence from *P. eryngii* peroxidase PS1 (mature protein) corresponding to the three-dimensional model built (details in Figs. 4 and 6), together with sequences from *P. chrysosporium* LiP (isoenzymes H8 and H2) and MnP1, and *Coprinus* ARP-CIP used for homology modeling.** The atomic coordinates of the four latter proteins were used as templates to obtain the three-dimensional model (Protein Data Bank entry 1BQW) for the *P. eryngii* peroxidase PS1 including two helical domains, which contain all the catalytically important residues (the C-terminal region, which has variable length in different peroxidases, was not modeled). The alignment was built by PILEUP from GCG package, and the amino acid residues identical to those found in the PS1 sequence are depicted in *white on black* (the distal and proximal histidine residues are marked with an *asterisk*). The position of the 12 helices in the PS1 peroxidase predicted by the DSSP program is indicated on the corresponding sequence. The mature ARP-CIP includes an extra N-terminal sequence of 8 amino acids (QGPGGGGS), which in other fungal peroxidases corresponds to the signal peptide.

square distance between backbone C_α with the LiP-H8 and ARP-CIP models. However, when superimposed with *P. chrysosporium* MnP1 differences were found in two superficial loops (PS1 Thr^{57}-Ala^{59} and MnP1 Leu^{228}-Thr^{234}).

Some aspects of the model directly related to catalytic activity were considered more in depth. The amino acid residues at the heme pocket of *P. eryngii* peroxidase PS1 were the same found in other fungal peroxidases (with the only exception of ARP-CIP): Arg^{43}, Phe^{46}, His^{47}, Glu^{78}, and Asn^{84} in the distal side and His^{175}, Phe^{192} (Leu^{201} in ARP-CIP), and Asp^{237} in the proximal side. Fig. 4 (*left side*) shows the opening of the main heme access channel in *P. eryngii* peroxidase PS1 (*top*), *P. chrysosporium* LiP-H8 (*center*), and MnP1 (*bottom*). This channel enables the access of hydroperoxides to the distal side of heme. Moreover, it has been postulated that some of the edge residues are involved in oxidation of aromatic substrates by LiP and horseradish peroxidase. As shown in Fig. 4, the *P. eryngii* peroxidase PS1 conserves six of the eight residues delimiting the channel edge in LiP-H8 (and one of the two differences is the substitution of Ile^{85} by Leu^{85}). However, the heme channel of *P. chrysosporium* MnP1 differs from that of LiP-H8 in five residues. Fig. 4 (*right side*) also shows the narrow Mn^{2+} channel of *P. eryngii* peroxidase PS1 and *P. chrysosporium* MnP1 directly on the internal heme propionate, where the cation is fixed by the three acidic amino acid residues (one aspartate and two glutamates) delimiting the channel edge. Finally, it is interesting that Trp^{170} of peroxidase PS1 occupies a position at the protein surface similar to that of LiP Trp^{171} (that could transfer electrons to heme because of topological proximity), whereas a similar residue is absent from the ARP-CIP and MnP1 models.

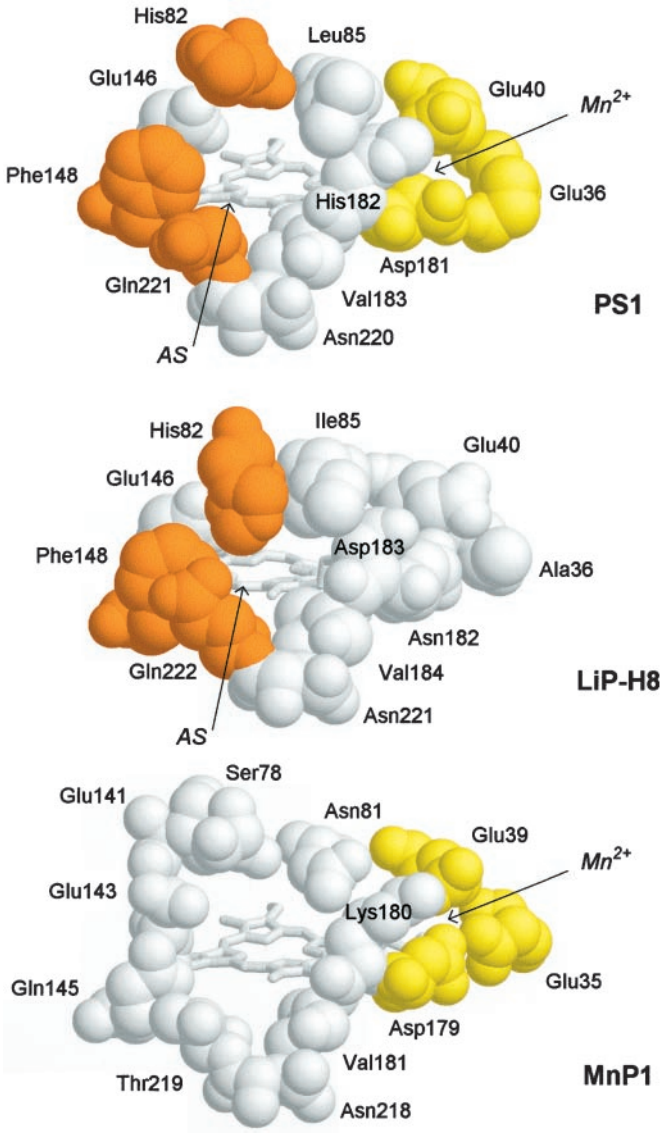

FIG. 4. **Amino acid residues at the opening of the main heme-channel of *P. chrysosporium* LiP-H8 reported to be involved in aromatic substrate (*AS*) oxidation (*center*) and residues forming the small Mn^{2+} channel of *P. chrysosporium* MnP1 (*bottom*) compared with residues occupying the same positions in *P. eryngii* peroxidase PS1 (*top*) (as van der Waals' spheres).** The three acidic residues responsible for Mn^{2+} binding are indicated in *yellow*. His^{82} and $Gln^{221/222}$, reported as involved in veratryl alcohol binding to LiP (His^{82} also in electron transfer to heme; see Fig. 6), and Phe^{148}, occupying a position similar to that of horseradish peroxidase Phe^{142} involved in aromatic substrate interaction, are indicated in *orange*. The atomic coordinates correspond to Brookhaven Protein Data Base entries 1BQW (three-dimensional model for peroxidase PS1 built from sequence in Fig. 3, modeled without Mn^{2+}), 1LLP, and 1MNP (LiP-H8 and MnP1 crystal models).

DISCUSSION

LiP and MnP of *P. chrysosporium* have been considered as two models for all ligninolytic peroxidases. However, this study shows that one of the two major peroxidases produced by *P. eryngii* during lignin degradation under natural growth conditions can be considered as representative for a third type of ligninolytic peroxidase, different from other microbial, plant, or animal peroxidases (17). As shown in Fig. 5, this versatile peroxidase is able to perform both the oxidative reactions characteristic of *P. chrysosporium* LiP, *i.e.* the oxidation of nonphenolic aromatic substrates *via* aromatic radicals, and MnP, *i.e.* the oxidation of Mn^{2+} to Mn^{3+}. Its affinity for H_2O_2 and Mn^{2+} was higher than reported for *P. chrysosporium* peroxidases, but the turnover number for Mn^{2+} and the affinity and turnover number for veratryl alcohol were lower (32–34). Moreover, the *P. eryngii* peroxidase efficiently oxidizes substituted phenols (the affinity for methoxyhydroquinones being even higher than for Mn^{2+}), which cannot be oxidized by the *P. chrysosporium* peroxidases. This is because these compounds inactivate LiP in the absence of veratryl alcohol (31), whereas compound II of *P. chrysosporium* MnP needs to be reduced by Mn^{2+} to close the catalytic cycle (phenols are indirectly oxidized by Mn^{3+}) (35). In addition to the above substrates, the *P. eryngii* peroxidase PS1 can oxidize two compounds, α-keto-γ-methylthiobutyric acid and *p*-dimethoxybenzene, which were those used for LiP detection (7) and for demonstration of oxidation mechanism by this enzyme (36). The oxidation of α-keto-γ-methylthiobutyric acid, a substrate characteristic of strong one-electron abstracting agents (such as LiP and hydroxyl radical), to ethylene by peroxidase PS1 has been reported very recently (37). The results of *p*-dimethoxybenzene oxidation to benzoquinone confirmed that the *P. eryngii* peroxidase has high redox potential and acts on aromatic substrates by the same mechanism described for LiP, *i.e. via* an aromatic cation radical formed by one electron oxidation of the benzenic ring (36). Finally, Reactive Black 5 is oxidized by the *P. eryngii* peroxidase, the reaction being inhibited by high Mn^{2+} concentrations. This azo dye cannot be oxidized by *P. chrysosporium* MnP because its redox potential is higher than that of Mn^{3+} tartrate nor by LiP in the absence of veratryl alcohol because of rapid inactivation (38). However, no inactivation is produced in the case of peroxidase PS1. The Reactive Black 5 also acts as a very efficient noncompetitive inhibitor of Mn^{2+} oxidation by the *P. eryngii* peroxidase. This result agrees with the noncompetitive inhibition by Mn^{2+} of the oxidation of dyes and veratryl alcohol by two similar peroxidases recently isolated from liquid cultures of *Pleurotus* and *Bjerkandera* species (38–40) and supports the existence in these proteins

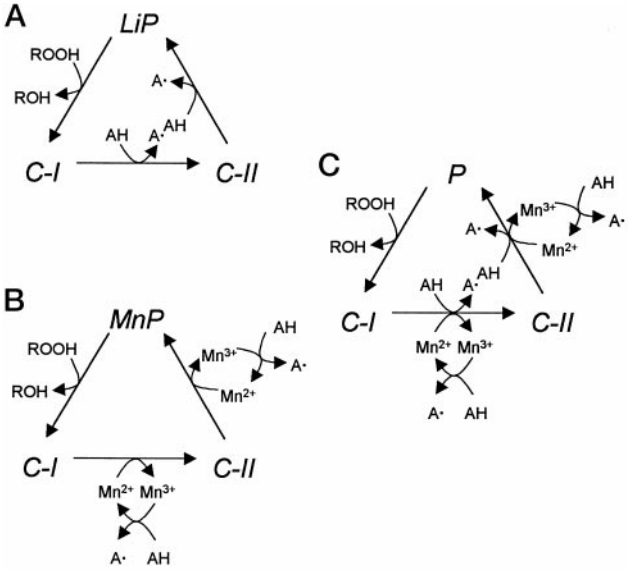

FIG. 5. **Scheme of catalytic cycles of *P. chrysosporium* LiP (*A*) and MnP (*B*) compared with *Pleurotus* peroxidase (*C*) (*panels A* and *B* were adapted from Ref. 13).** Cycles include two-electron oxidation of enzyme by hydroperoxides (ROOH) to compound I, a complex of high valent oxo-iron and porphyrin cation radical ([Fe^{4+} = O P^{+}]), followed by two one-electron reductions of compound I to compound II ([Fe^{4+} = O P]) and native enzyme ([Fe^{3+} P]), producing two oxidations of the electron donor. They differ in electron donors, which can be: (i) aromatic compounds (*AH*) for LiP (generally nonphenolic because the enzyme is inactivated during oxidation of phenols); (ii) Mn^{2+} for MnP (although phenols can reduce compound I and are indirectly oxidized by Mn^{3+}); and (iii) Mn^{2+} and phenolic or nonphenolic aromatic compounds for the *Pleurotus* peroxidase. The optimum for Mn^{2+} oxidation in all above reactions was around pH 5, and that for direct oxidation of aromatic substrate was around pH 3.

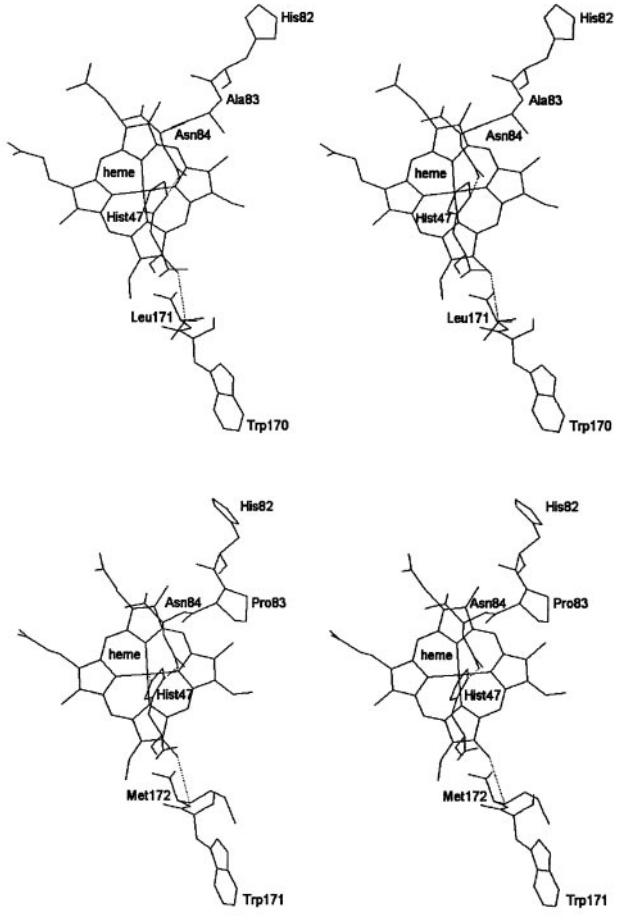

FIG. 6. **Stereo views showing two hypothetical LRET pathways to heme in *P. eryngii* peroxidase PS1 (*top*) and *P. chrysosporium* LiP isoenzyme H8 (*bottom*) from His^{82} at heme-channel edge (*via* distal His) and from PS1 Trp^{170} or LiP Trp^{171}.** The atomic coordinates correspond to Brookhaven Protein Data Base entries 1LLP (LiP-H8 crystal model) and 1BQW (three-dimensional model for peroxidase PS1 built from the sequence in Fig. 3).

of a specific substrate interaction site for Mn^{2+}, different from that involved in oxidation of other peroxidase substrates.

No crystal structures for *P. chrysosporium* LiP have been obtained containing veratryl alcohol, which would provide invaluable information for identification of substrate interaction site. However, when the enzyme was crystallized (14, 15),it was suggested that oxidation of veratryl alcohol could be produced at the heme access channel, and some amino acid residues were postulated to be involved in substrate binding and electron transfer. Poulos *et al.* (14) modeled the veratryl alcohol molecule at the heme edge of LiP-H8, H-bonded to His^{82} and Gln^{222}. These two residues are conserved in the *P. eryngii* peroxidase PS1, which has a remarkably similar heme access channel as shown in the three-dimensional model obtained (Fig. 4, *top* and *center*). The presence of different amino acid residues at the above two positions (Fig. 4, *bottom*) probably prevents direct oxidation of aromatic substrates by MnP, together with other differences resulting in a more polar channel environment. It is interesting that Phe^{142} of horseradish peroxidase, which occupies a position similar to that of Phe^{148} of *P. eryngii* peroxidase and LiP-H8, has been reported to be involved in aromatic substrate interaction (41, 42). Despite the possibility of direct electron transfer from veratryl alcohol at the above binding site to heme as was postulated in *P. chrysosporium* LiP, substrate oxidation *via* long range electron transfer (LRET) should also be considered taking into account the distance between channel opening and heme edge. This was suggested by Schoemaker *et al.* (43), who proposed one of the LRET pathway shown in Fig. 6 (*bottom*). This initiates in LiP His^{82}, mentioned as involved in veratryl alcohol binding, and proceeds *via* Pro^{83} and Asn^{84}, the latter being H-bonded to the distal histidine (His^{47}). Such a LRET pathway does not exist in *P. chrysosporium* MnP, but the three-dimensional model built showed that the His^{82} of *P. eryngii* peroxidase was also exposed at the heme channel opening (Fig. 4, *top*) and connected by a similar pathway with the distal histidine (PS1 His^{47}) (Fig. 6, *top*). The difference is that PS1 Ala^{83} occupies the position of LiP Pro^{83}, resulting in a different position of His^{82} side chain at the protein surface. Recently Trp^{171} of *P. chrysosporium* LiP has been described as being involved in the catalytic cycle of the enzyme *via* a different LRET pathway (Fig. 6, *bottom*), which does not exist in *P. chrysosporium* MnP (44). However, Trp^{170} of *P. eryngii* peroxidase PS1 occupies a similar position at the protein surface and it is linked to heme by a LRET pathway as described in LiP (Fig. 6, *top*). Therefore, this aromatic residue could be involved in oxidation of some substrates by peroxidase PS1, whereas other substrates would be oxidized at the heme channel, as recently shown for *P. chrysosporium* LiP (45).

The ability to directly oxidize Mn^{2+} to Mn^{3+} is a unique characteristic of Mn^{2+}-oxidizing peroxidases produced by *P. chrysosporium* and many other white rot fungi (46). Other enzymes could oxidize Mn^{2+} *via* superoxide anion radical, such as that generated by redox cycling (47). The existence of a Mn^{2+} binding site in *P. chrysosporium* MnP was predicted in theoretical models of the enzyme built by sequence homology using LiP as a template (48), as well as in the first crystal structure obtained (16). Then it was indirectly confirmed by site-directed mutagenesis of MnP Glu^{35}, Glu^{39}, and Asp^{179} (32), and direct evidence obtained by x-ray diffraction of the enzyme crystal-

lized in the presence of Mn^{2+} (49). As shown in Fig. 4, the *P. eryngii* peroxidase PS1 has the same three acidic amino acid residues (Glu^{36}, Glu^{40}, and Asp^{181}) forming a small channel directly on the internal heme propionate that acts as first electron acceptor for Mn^{2+} oxidation by these peroxidases. The absence of the three above residues in *P. chrysosporium* LiP (Ala^{36}, Glu^{40}, and Asn^{182} at the corresponding positions) results in inability to bind and oxidize Mn^{2+} (Fig. 4, *center*). The pH optimum for oxidation of Mn^{2+} (pH 5) is higher than for direct oxidation of aromatic substrates (pH 3) by the *P. eryngii* peroxidase. This is because the three acidic residues and the internal heme propionate at the Mn^{2+} interaction site should be dissociated to bind the cation. The low pH for manganese-independent oxidations is probably due to increased redox potential of heme at low pH values, but the involvement of an acidic amino acid residue in its protonated form has also been suggested (14).

No typical LiP is produced by *Pleurotus* species, but several Mn^{2+}-oxidizing peroxidases have been reported. Those from *P. pulmonarius* cultures on wheat straw (18) and *P. ostreatus* on sawdust (MnP2) (50) probably correspond to the same peroxidase described here, because they have the same N-terminal sequence and catalytic properties. Peroxidases similar to that produced by *P. eryngii* in liquid culture (GenBank accession number AF007223 and its allelic variant AF007224) (23, 51) are produced by *P. pulmonarius* in liquid culture (18) and by *P. ostreatus* in both liquid (52) and sawdust cultures (MnP1) (50) (N terminus ATCADGRTT). In addition to these peroxidases oxidizing both Mn^{2+} and aromatic substrates and dyes, the peroxidase PS3 from *P. eryngii* and a peroxidase from liquid culture of *P. ostreatus* (53) (differing in N terminus) are closer to *P. chrysosporium* MnP. Production of specific isoenzymes on natural substrates has also been reported in other fungi (18–20), but the physiological/ecological significance of the different peroxidase isoenzymes remains to be established. Recently a MnP with some manganese-independent activity has been described in *Poria* (synonym: *Ceriporiopsis*) *subvermispora* (54), but it has low sequence homology with *P. eryngii* peroxidases and is not able to oxidize veratryl alcohol. However, enzymes with catalytic properties similar to *Pleurotus* versatile peroxidases (23) have been found in *Bjerkandera adusta* (55) and *Bjerkandera* sp. (40), the latter being described as a MnP-LiP "hybrid" enzyme. Some aspects of the three-dimensional model shown here suggests that the catalytic properties of this third type of ligninolytic peroxidase are related to a hybrid molecular structure including MnP and LiP-type features. Site-directed mutagenesis studies are necessary to confirm substrate interaction sites and LRET pathways (as proposed from His^{82} and Trp^{170}) in *P. eryngii* peroxidases. This will be facilitated by the recent expression in *Emericella nidulans* of the gene encoding a *P. eryngii* peroxidase.

Acknowledgments—We thank L. Caramelo (Sigma-Aldrich, Spain) for stimulating discussions about LiP-type peroxidases, F. Guillén for help in quinone analyses, B. Böckle for contribution to kinetic constant determination, A. Heinfling (Technical University of Berlin, Germany) for a sample of Reactive Black 5, and J. A. Field (Wageningen Agricultural University, The Netherlands) for information about *Bjerkandera* sp. peroxidases. S. S. acknowledges the European Fellowship (Human Capital and Mobility programme) for supporting his stage at Centro de Investigaciones Biológicas. We thank J. Varela for N-terminal sequencing, A. Díaz for DNA sequencing, and A. Guijarro and T. Raposo for technical assistance.

REFERENCES

1. Steinlin, H. (1979) in *Holz als Rohstoff in der Weltwirtschaft* (Plochmann, R., and Löffler, H., eds) pp. 14–44, Landwirtschaftsverlag, Münster, Germany
2. Higuchi, T. (1997) *Biochemistry and Molecular Biology of Wood*, Springer Verlag, London
3. Kirk, T. K., and Farrell, R. L. (1987) *Annu. Rev. Microbiol.* **41,** 465–505
4. Faison, B. D., and Kirk, T. K. (1983) *Appl. Environ. Microbiol.* **46,** 1140–1145
5. Tien, M., and Kirk, T. K. (1983) *Science* **221,** 661–663
6. Glenn, J. K., Morgan, M. A., Mayfield, M. B., Kuwahara, M., and Gold, M. H. (1983) *Biochem. Biophys. Res. Commun.* **114,** 1077–1083
7. Kuwahara, M., Glenn, J. K., Morgan, M. A., and Gold, M. H. (1984) *FEBS Lett.* **169,** 247–250
8. Martínez-Iñigo, M. J., and Kurek, B. (1997) *Holzforschung* **51,** 543–548
9. Bao, W. L., Fukushima, Y., Jensen, K. A., Moen, M. A., and Hammel, K. E. (1994) *FEBS Lett.* **354,** 297–300
10. Schoemaker, H. E., Lundell, T. K., Hatakka, A. I., and Piontek, K. (1994) *FEMS Microbiol. Rev.* **13,** 321–332
11. Gold, M. H., and Alic, M. (1993) *Microbiol. Rev.* **57,** 605–622
12. Shimada, M., and Higuchi, T. (1991) in *Wood and Cellulosic Chemistry* (Hon, D. N. S., and Shiraishi, N., eds) pp. 557–619, Marcel Dekker, New York
13. Eriksson, K.-E. L., Blanchette, R. A., and Ander, P. (1990) *Microbial and Enzymatic Degradation of Wood Components*, Springer-Verlag, Berlin, Germany
14. Poulos, T. L., Edwards, S. L., Wariishi, H., and Gold, M. H. (1993) *J. Biol. Chem.* **268,** 4429–4440
15. Piontek, K., Glumoff, T., and Winterhalter, K. (1993) *FEBS Lett.* **315,** 119–124
16. Sundaramoorthy, M., Kishi, K., Gold, M. H., and Poulos, T. L. (1994) *J. Biol. Chem.* **269,** 32759–32767
17. Banci, L. (1997) *J. Biotechnol.* **53,** 253–263
18. Camarero, S., Böckle, B., Martínez, M. J., and Martínez, A. T. (1996) *Appl. Environ. Microbiol.* **62,** 1070–1072
19. Vares, T., Kalsi, M., and Hatakka, A. (1995) *Appl. Environ. Microbiol.* **61,** 3515–3520
20. Datta, A., Bettermann, A., and Kirk, T. K. (1991) *Appl. Environ. Microbiol.* **57,** 1453–1460
21. Martínez, A. T., Camarero, S., Guillén, F., Gutiérrez, A., Muñoz, C., Varela, E., Martínez, M. J., Barrasa, J. M., Ruel, K., and Pelayo, M. (1994) *FEMS Microbiol. Rev.* **13,** 265–274
22. Camarero, S., Barrasa, J. M., Pelayo, M., and Martínez, A. T. (1998) *J. Pulp Paper Sci.* **24,** 197–203
23. Martínez, M. J., Ruiz-Dueñas, F. J., Guillén, F., and Martínez, A. T. (1996) *Eur. J. Biochem.* **237,** 424–432
24. Muñoz, C., Guillén, F., Martínez, A. T., and Martínez, M. J. (1997) *Appl. Environ. Microbiol.* **63,** 2166–2174
25. Tappi (1993) *Test Methods 1992–1993*, TAPPI, Atlanta, GA
26. Petersen, J. F. W., Kadziola, A., and Larsen, S. (1994) *FEBS Lett.* **339,** 291–296
27. Kunishima, N., Fukuyama, K., Matsubara, H., Hatanaka, H., Shibano, Y., and Amachi, T. (1994) *J. Mol. Biol.* **235,** 331–344
28. Martínez, A. T., Ruiz-Dueñas, F. J., Sarkar, S., and Martínez, M. J. (1997) in *Resùmenes XVI Congreso de la Sociedad Española de Microbiología*, p. 89, Ultramar, Barcelona, Spain
29. Peitsch, M. C. (1996) *Biochem. Soc. Trans.* **24,** 274–279
30. Kabsch, W., and Sander, C. (1983) *Biopolymers* **22,** 2577–2637
31. Harvey, P. J., and Palmer, J. M. (1990) *J. Biotechnol.* **13,** 169–179
32. Kishi, K., Kusters-van Someren, M., Mayfield, M. B., Sun, J., Loehr, T. M., and Gold, M. H. (1996) *Biochemistry* **35,** 8986–8994
33. Glumoff, T., Harvey, P. J., Molinari, S., Goble, M., Frank, G., Palmer, J. M., Smit, J. D. G., and Leisola, M. S. A. (1990) *Eur. J. Biochem.* **187,** 515–520
34. Farrell, R. L., Murtagh, K. E., Tien, M., Mozuch, M. D., and Kirk, K. T. (1989) *Enzyme Microb. Technol.* **11,** 322–328
35. Glenn, J. K., Akileswaran, L., and Gold, M. H. (1986) *Arch. Biochem. Biophys.* **251,** 688–696
36. Kersten, P. J., Kalyanaraman, B., Hammel, K. E., Reinhammar, B., and Kirk, T. K. (1990) *Biochem. J.* **268,** 475–480
37. Caramelo, L., Martínez, M. J., and Martínez, A. T. (1998) *Appl. Environ. Microbiol.* **65,** 916–922
38. Heinfling, A., Ruiz-Dueñas, F. J., Martínez, M. J., Bergbauer, M., Szewzyk, U., and Martínez, A. T. (1998) *FEBS Lett.* **428,** 141–146
39. Heinfling, A., Martínez, M. J., Martínez, A. T., Bergbauer, M., and Szewzyk, U. (1998) *Appl. Environ. Microbiol.* **64,** 2788–2793
40. Mester, T., and Field, J. A. (1998) *J. Biol. Chem.* **273,** 15412–15417
41. Veitch, N. C., Williams, R. J. P., Bone, N. M., Burke, J. F., and Smith, A. T. (1995) *Eur. J. Biochem.* **233,** 650–658
42. Gajhede, M., Schuller, D. J., Henriksen, A., Smith, A. T., and Poulos, T. L. (1997) *Nat. Struct. Biol.* **4,** 1032–1038
43. Schoemaker, H. E., Lundell, T. K., Floris, R., Glumoff, T., Winterhalter, K. H., and Piontek, K. (1994) *Bioorg. Med. Chem.* **2,** 509–519
44. Blodig, W., Doyle, W. A., Smith, A. T., Winterhalter, K., Choinowski, T. H., and Piontek, K. (1998) *Biochemistry* **37,** 8832–8838
45. Doyle, W. A., Blodig, W., Veitch, N. C., Piontek, K., and Smith, A. T. (1998) *Biochemistry* **37,** 15097–15105
46. Hatakka, A. (1994) *FEMS Microbiol. Rev.* **13,** 125–135
47. Guillén, F., Martínez, M. J., Muñoz, C., and Martínez, A. T. (1997) *Arch. Biochem. Biophys.* **339,** 190–199
48. Johnson, F., Loew, G. H., and Du, P. (1994) *Protein Struct. Funct. Genet.* **20,** 312–319
49. Sundaramoorthy, M., Kishi, K., Gold, M. H., and Poulos, T. L. (1997) *J. Biol. Chem.* **272,** 17574–17580
50. Palmieri, G., Giardina, P., Zocchi, I., and Sannia, G. (1998) in *Proceedings of the 7th International Conference on Bio/Technology in the Pulp and Paper Industry, June 16–19, 1998, Vancouver, British Columbia, Canada*, pp. B253–B256, Canadian Pulp and Paper Association, Montreal, Canada
51. Ruiz-Dueñas, F. J., Martínez, M. J., and Martínez, A. T. (1998) *Mol. Microbiol.* **31,** 223–236
52. Sarkar, S., Martínez, A. T., and Martínez, M. J. (1997) *Biochim. Biophys. Acta* **1339,** 23–30
53. Asada, Y., Watanabe, A., Irie, T., Nakayama, T., and Kuwahara, M. (1995) *Biochim. Biophys. Acta* **1251,** 205–209
54. Lobos, S., Larrondo, L., Salas, L., Karahanian, E., and Vicuña, R. (1998) *Gene* (*Amst.*) **206,** 185–193
55. Heinfling, A., Martínez, M. J., Martínez, A. T., Bergbauer, M., and Szewzyk, U. (1998) *FEMS Microbiol. Lett.* **165,** 43–50

Description of a Versatile Peroxidase Involved in the Natural Degradation of Lignin That Has Both Manganese Peroxidase and Lignin Peroxidase Substrate Interaction Sites

Susana Camarero, Sovan Sarkar, Francisco Javier Ruiz-Dueñas, Mari?a Jesús Marti?nez and Ángel T. Marti?nez

J. Biol. Chem. 1999, 274:10324-10330.
doi: 10.1074/jbc.274.15.10324